



High-resolution mid-IR spectrometer based on frequency upconversion

Hu, Qi; Dam, Jeppe Seidelin; Pedersen, Christian; Tidemand-Lichtenberg, Peter

Published in:
Optics Letters

Link to article, DOI:
[10.1364/OL.37.005232](https://doi.org/10.1364/OL.37.005232)

Publication date:
2012

Document Version
Publisher's PDF, also known as Version of record

[Link back to DTU Orbit](#)

Citation (APA):

Hu, Q., Dam, J. S., Pedersen, C., & Tidemand-Lichtenberg, P. (2012). High-resolution mid-IR spectrometer based on frequency upconversion. *Optics Letters*, 37(24), 5232-5234. <https://doi.org/10.1364/OL.37.005232>

General rights

Copyright and moral rights for the publications made accessible in the public portal are retained by the authors and/or other copyright owners and it is a condition of accessing publications that users recognise and abide by the legal requirements associated with these rights.

- Users may download and print one copy of any publication from the public portal for the purpose of private study or research.
- You may not further distribute the material or use it for any profit-making activity or commercial gain
- You may freely distribute the URL identifying the publication in the public portal

If you believe that this document breaches copyright please contact us providing details, and we will remove access to the work immediately and investigate your claim.

High-resolution mid-IR spectrometer based on frequency upconversion

Qi Hu, Jeppe Seidelin Dam, Christian Pedersen, and Peter Tidemand-Lichtenberg*

DTU Fotonik, Technical University of Denmark, Roskilde DK-4000, Denmark

*Corresponding author: ptli@fotonik.dtu.dk

Received September 18, 2012; revised November 5, 2012; accepted November 5, 2012;
posted November 7, 2012 (Doc. ID 176426); published December 13, 2012

We demonstrate a novel approach for high-resolution spectroscopy based on frequency upconversion and postfiltering by means of a scanning Fabry–Perot interferometer. The system is based on sum-frequency mixing, shifting the spectral content from the mid-infrared to the near-visible region allowing for direct detection with a silicon-based CCD camera. This approach allows for low noise detection even without cooling of the detector. A setup is realized for the 3 μm regime with a spectral resolution of 0.2 nm using lithium niobate as the nonlinear material and mixing with a single-frequency 1064 nm laser. We investigate water vapor emission lines from a butane burner and compare the measured results to model data. The presented method we suggest to be used for real-time monitoring of specific gas lines and reference signals. © 2012 Optical Society of America

OCIS codes: 300.6340, 190.4360, 230.7405.

In the past years there has been a lot of attention directed toward infrared spectroscopy. Particularly the mid-infrared (mid-IR) spectral region has been studied intensively, as many gasses have their fundamental absorption lines in this region. Although many potential applications have emerged, commercial applications have been somewhat limited by the lack of efficient, high-resolution, low-cost, mid-IR spectrometers with high sensitivity [1].

High-resolution mid-IR spectroscopy is used for a wealth of applications, reaching from breath analysis [2], combustion analysis [3] to monitoring of atmospheric changes [4], as well as applications within security and defense [5].

Today, the method of choice for obtaining infrared spectra is Fourier transform infrared spectroscopy (FTIR). FTIR is the optimal choice when the detector noise is the dominant noise source [6]. However, in order to obtain high spectral resolution, FTIR requires translation of a mirror over several centimeters. The long scanning range limits the temporal performance and adds significantly to system complexity and costs.

In the visible and near-infrared range spectrometers and optical spectrum analyzers are in widespread use.

In this Letter, we demonstrate an approach based on shifting of the spectrum from the mid-IR region to the detector wise more developed near visible spectral region. The frequency shift is obtained by sum-frequency mixing with a single-frequency laser, resulting in a simple shift of the center frequency, while maintaining the spectral content for subsequent detection. Nonlinear conversion for frequency shifting has traditionally been considered inefficient, however, recently high conversion efficiencies has been shown even for incoherent infrared radiation [7] reaching quantum efficiencies of 20%.

The frequency conversion process depends strongly on the phase-match condition; hence, only a limited spectral region is upconverted for a given direction of propagation through the nonlinear material. The spectral resolution resulting from the phase-match condition is relatively low. However, it is straightforward to improve resolution by means of a scanning Fabry–Perot

interferometer postprocessing the upconverted radiation before detection. In this Letter, a planar high finesse two-mirror interferometer is used to make narrow filtering of the upconverted radiation.

The system performance is demonstrated by measurements of the spectral emission from hot water vapor associated with a butane flame. The measured spectrum is found to correspond to spectral data calculated from the commercial HITEMP database using SpectralCalc [8].

In this work, the incoming signal wavelength of 2.85 to 5 μm is shifted to the 775 to 880 nm region by sum-frequency mixing with a single-frequency 1064 nm laser. See Fig. 1 for the schematic system layout.

In the present setup, a butane burner is used as a light source, measuring the emission from the hot water vapor associated with the combustion of butane. A single point of the flame is imaged by a dual lens system ($f_1 = 40$ mm and $f_2 = 70$ mm), through a germanium window (Ge) to remove visible light, into the frequency conversion device. Since the dark noise generated by the conversion process is negligible [7], the method can be used for any range of light source powers, provided that all exterior light sources have been adequately reduced. Only the exposure time needs to match the analyzed spectral radiance levels.

The frequency conversion takes place in a 20 mm long periodically poled LiNbO₃ crystal (PP:LN) with a poling period of 21 μm . The PP:LN crystal is placed in a large beam waist (180 μm) intracavity in a single-frequency unidirectional 1064 nm Nd:YVO₄ laser with a circulating power of approximately 8 W. The circulating power and wavelength is very stable.

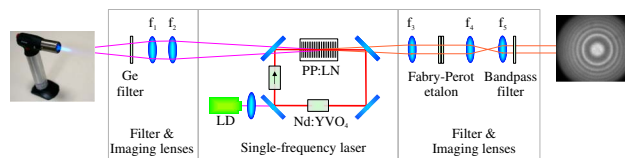


Fig. 1. (Color online) Schematic layout of the setup. The signal is imaged through the frequency converter and filtered by the scanning Fabry–Perot. The output is captured by a standard CCD camera in the 800 nm spectral range.

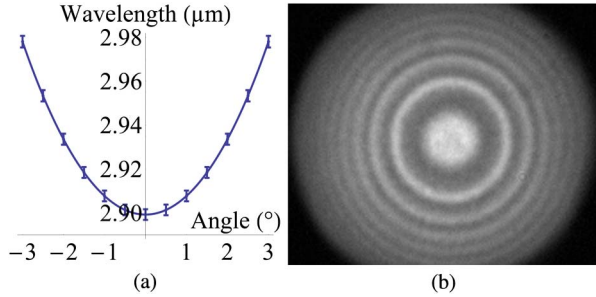


Fig. 2. (Color online) (a) Phase-match curve along with the acceptance bandwidth of the nonlinear conversion process. Error bars indicate phase-matched bandwidth. (b) The upconverted image of mid-IR emission from hot water vapor at 2.9 μm .

Varying the temperature of the PP:LN crystal between 30°C and 200°C results in possible collinear phase match from 2.85 to 3.04 μm . Other wavelengths can be reached using different poling periods.

The phase-match condition of the upconversion process depends on the angle of propagation through the converter, relative to the direction of the mixing laser. Hence, the upconverted radiation has a radial intensity distribution corresponding to the spectral content of the signal, as seen in Fig. 2. Figure 2(a) shows the theoretical correlation between the spectral content and the radial position in the upconverted image originating from the phase-match condition.

The output from the mixing device is collimated by a single lens ($f_3 = 150$ mm) and scaled by a 4-f imaging system ($f_4 = 100$ mm and $f_5 = 30$ mm) onto an EM-CCD camera (Andor Luca S).

The acceptance bandwidth of the nonlinear conversion is approximately 5 nm near 3 μm and increases when approaching 4.2 μm , as indicated by the bars on Fig. 2(a). This results in a comparatively low spectral resolution, limited only by the acceptance parameters of the nonlinear process. It is now straightforward to obtain the spectrum of the light source by a simple radial analysis of the image. The result of this analysis is shown as the low spectral resolution graph in Fig. 3(a).

Improved spectral resolution can be reached by insertion of a planar high-finesse scanning Fabry–Perot interferometer in the collimated beam after the lens, f_3 , as indicated in Fig. 1

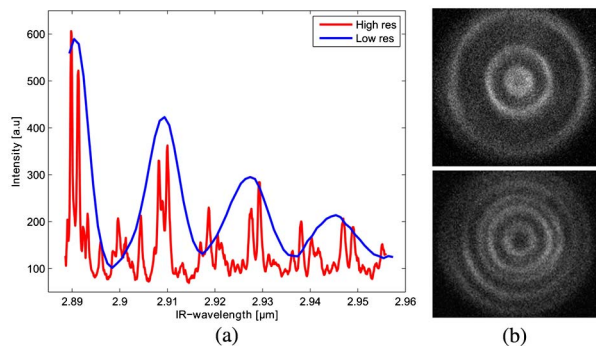


Fig. 3. (Color online) (a) Low and high spectral resolution of the same water vapor emission lines. (b) CCD images for two different Fabry–Perot mirror spacings. (Media 1 showing images scanning the mirror spacing clicking the CCD images.)

The inclusion of the high-finesse interferometer in the upconverted signal, removes the spectral components outside the transmission peaks of the Fabry–Perot. This imposes two simultaneous conditions on the imaged wavelengths, one from the phase-match condition for efficient conversion and one from the transmission characteristic of the interferometer.

The interferometer is designed to have a free spectral range (FSR) larger than the acceptance bandwidth of the nonlinear conversion. This means that the upconverted image consists of spatially separate rings in increments of the FSR.

Comparing two images acquired at slightly different mirror spacing's of the interferometer, a clear difference is seen in the transmitted radiation. The images in Fig. 3(b) are acquired with an interferometer voltage of 7.0 and 8.4 V, respectively, where a voltage difference of 8.1 V corresponds to one full FSR. Admittedly, the images may appear noisy (shot noise is apparent). However, since the data analysis averages the spectrum over a full circle this noise is averaged out.

The high-resolution spectrum, calculated from the filtered images, is shown in Fig. 3(a) together with the low-resolution spectrum. It is clearly seen, that the scanning interferometer improves the spectral resolution. However, it is important to note, that the interferometer needs to be inserted in a collimated geometry, with a sufficiently large Rayleigh range of the upconverted radiation to allow the ring pattern to pass through the interferometer (considering its length and finesse) without affecting the point spread function (PSF) of the imaging system. Particularly, the collimating lens, f_3 , is chosen to achieve sufficient Rayleigh length without overfilling the interferometer mirrors. The interferometer is placed in a 2-f geometry relative to the nonlinear crystal, to ensure the collimated geometry.

The amount of rings that can be distinguished after filtering is ultimately limited by the PSF from the imaging process [9]. Since the rings are located closer and closer as their radii grow, the PSF limits the amount of discernible rings.

Using a larger diameter of the mixing laser (decreasing the PSF), more rings would be discernible. However, at the same time, this would require a larger focal length of the collimating lens, f_3 , in order to maintain the Rayleigh range at the interferometer plane. This would in turn overfill the interferometer, and thus the additional rings would be lost unless larger diameter interferometer mirrors were used. Obviously, these counteracting requirements necessitate a careful design of the optical geometry.

Furthermore, as seen from Fig. 3, the intensity of the spectral features seems to decrease moving away from the center of the image. This is an artifact from the decreasing width of the rings and blurring by the PSF, which is easily compensated by postprocessing.

High-resolution spectra has been acquired for three different temperatures of the PP:LN crystal. This way it is possible to select the region of interest and acquire the spectrum in each range by scanning of the interferometer. Figure 4 shows the measured high-resolution spectra compared to spectral data from hot water vapor emission calculated using the HITEMP database in the

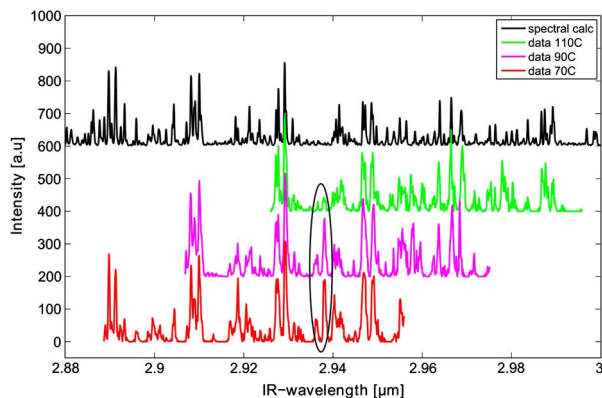


Fig. 4. (Color online) Measured high resolution spectra for three different crystal temperatures compared to spectral data calculated from HITEMP database using SpectralCalc [8]. The reference emission spectrum is calculated at 1500 K, and atmospheric pressure.

SpectralCalc software [8] with a spectral resolution of 0.2 nm. The butane flame of course also contains other hot gasses like CO_2 , but none of these have emission in the analyzed spectral range and can thus be ignored. In the measured data the decreasing intensity moving away from the center of the image has been compensated as mentioned above.

As seen from the measurements, the overlapping parts of the spectrum from the three different temperatures match well with each other, as well as with the theoretical spectrum for water vapor emission, especially for the central part of the images. As you move away from the central part of the image, resolution deteriorates and false peaks start to appear as indicated by the black ellipse in the lower spectra. This peak is not present in the theoretical nor in the measured spectra with highest phase-match temperature. The reason for this discrepancy is, that the FSR of the interferometer is not quite large enough compared to the combined effect of the PSF (which is constant in the entire image) and the spectral dependence of the angular position in the image. It is reminded, that the equidistantly spaced spectral components in the water vapor emission results in denser ring patterns moving away from the collinear regime in the center of the image, as clearly seen in Fig. 2.

To optimize the resulting spectral resolution, we have applied a Wiener filter (mathematical deconvolution in postprocessing) to the obtained data shown in Fig. 4. This improved the spectral resolution from approximately 0.45 to 0.2 nm. The unfiltered resolution is determined by the ratio of the FSR and the finesse of the interferometer. Using a higher finesse interferometer it would be possible to obtain even better spectral resolution.

The center wavelength of the spectrometer is calibrated by a known IR light source [10].

While the presented device is built on an optical table, it could easily be integrated into a portable device similar to the system presented in [7]. This would eliminate background signals from room lighting and pump laser, thus increasing the sensitivity to the single photon level in the mid-IR. Additionally, the interferometer would filter away a large part of the system-generated noise, leaving real-time photon counting spectral performance in the mid-IR.

A simple realization of this could be achieved by relaying the innermost circle to one photomultiplier counting the received photons, and one or more exterior circular regions to another photomultiplier to be used as reference signals.

In this work we have demonstrated a novel approach for high spectral resolution measurements of mid-IR radiation by means of upconversion and subsequent filtering with a planar scanning interferometer. The presented method is ideal for applications where monitoring of a specific gas line is required. By this method a single frame of the acquired light gives information about specific gas line, while the neighboring rings gives a reference signal. Using this method and considering the high sensitivity and low intrinsic noise of the principle [7], we believe that this sets a new standard for efficient monitoring of single gas lines.

Furthermore, using this method a full scan consists of moving the interferometer mirror approximately 400 nm, whereas to obtain similar resolution in FTIR, the mirror would need to be moved several centimeters. Of course this allows for much faster high-resolution spectral measurements even using an uncooled detector device. It is noted that the present system only has a circulating 1064 nm power of 8 W, resulting in an image acquisition time after Fabry–Perot filtering of 1 s. The circulating power can easily be scaled a factor of 10 resulting in a corresponding improvement in acquisition speed.

References

1. M. N. Abedin, M. G. Mlynczak, and T. F. Refaat, *Proc. SPIE* **7808**, 78080V (2010).
2. M. R. McCurdy, Y. Bakhirkin, G. Wysocki, R. Lewicki, and F. K. Tittel, *J. Breath Res.* **1**, 014001 (2007).
3. Z. W. Sun, M. Försth, Z. S. Li, B. Li, and M. Aldén, *Fire Mater.* **35**, 527 (2011).
4. J. Li, U. Parchatka, R. Königstedt, and H. Fischer, *Opt. Express* **20**, 7590 (2012).
5. L. Becker, *Proc. SPIE* **6127**, 61270S (2006).
6. P. R. Griffiths and J. A. de Haseth, *Fourier Transform Infrared Spectrometry*, 2nd ed. (Wiley, 2007).
7. J. S. Dam, P. Tidemand-Lichtenberg, and C. Pedersen, *Nat. Photonics* **6**, 788 (2012).
8. "Spectral Calculator—High resolution gas spectra," <http://www.spectralcalc.com/calc/spectralcalc.php>.
9. J. S. Dam, C. Pedersen, and P. Tidemand-Lichtenberg, *Opt. Express* **20**, 1475 (2012).
10. L. Høgstedt, O. B. Jensen, J. S. Dam, C. Pedersen, and P. Tidemand-Lichtenberg, *Laser Phys.* **22**, 1676 (2012).